

Using the expression found for  $E_y$  corresponding to (6) in the boundary conditions (5b) one obtains

$$\alpha_1 D_1 A_1 + \alpha_2 D_2 A_2 + \alpha_3 D_3 A_3 = 0 \quad (8a)$$

$$\begin{aligned} \alpha_1 D_1 A_1 \cos \alpha_1 a - \alpha_1 D_1 B_1 \sin \alpha_1 a + \alpha_2 D_2 A_2 \cos \alpha_2 a - \\ - \alpha_2 D_2 B_2 \sin \alpha_2 a + \alpha_3 D_3 A_3 \cos \alpha_3 a - \alpha_3 D_3 B_3 \sin \alpha_3 a = 0. \quad (8b) \end{aligned}$$

Using the expression found for  $u_x$  corresponding to (6) in the boundary conditions (5c) one obtains

$$A_1 P_1 + A_2 P_2 + A_3 P_3 = 0 \quad (9a)$$

$$\begin{aligned} A_1 P_1 \cos \alpha_1 a - B_1 P_1 \sin \alpha_1 a + A_2 P_2 \cos \alpha_2 a - B_2 P_2 \sin \alpha_2 a \\ + A_3 P_3 \cos \alpha_3 a - B_3 P_3 \sin \alpha_3 a = 0. \quad (9b) \end{aligned}$$

Equations (7), (8), and (9) represent six linear homogeneous equations with the six unknowns  $A_1, A_2, A_3$  and  $B_1, B_2, B_3$ , and for a nontrivial solution the determinant of the coefficients should be zero.

Substituting the values of  $\alpha_1(\gamma)$ ,  $\alpha_2(\gamma)$ , and  $\alpha_3(\gamma)$  found from (4) in the above determinantal equation, one obtains a transcendental determinantal equation for the propagation constant  $\gamma$  of the plasma waves hybrid modes. The solution of this equation will give an infinite number of discrete solutions for  $\gamma$ . For each  $\gamma$  of a particular hybrid mode, one may find the corresponding characteristic values  $\alpha_1$ ,  $\alpha_2$ , and  $\alpha_3$ , from which one is able to find the field components of the corresponding plasma wave hybrid mode.

#### REFERENCES

[1] H. Unz, "Propagation in transversely magnetized compressible plasma between two parallel planes," *IEEE Trans. Microwave Theory Tech.*, vol. MTT-30, pp. 894-899, June, 1982.

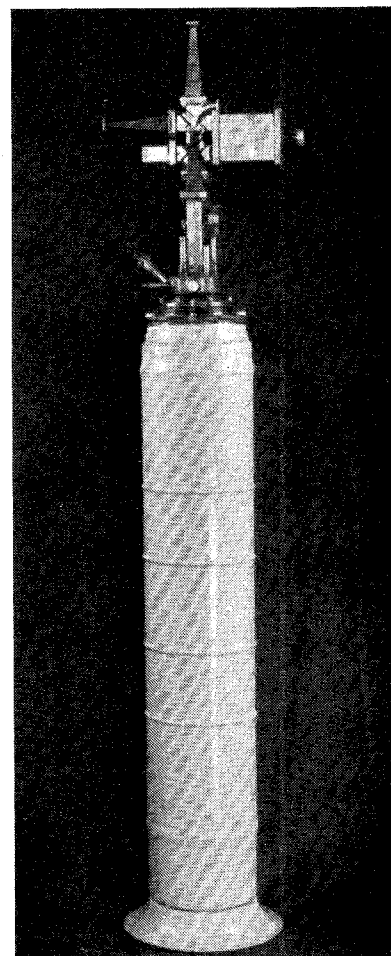


Fig. 1. General view of the maser.

## A Broad-Band Traveling-Wave Maser for the Range 40-46.5 GHz

NICKOLAY T. CHERPAK AND TAMARA A. SMIRNOVA

**Abstract** — A tunable traveling-wave maser (TWM) for the frequency range 40-46.5 GHz has been developed, which is characterized by an extended instantaneous bandwidth. Andalusite ( $\text{Al}_2\text{SiO}_5$ ) doped with  $\text{Fe}^{3+}$  atoms is used as the active crystal. The slow-wave structure is a digit comb with broad-band matching particularly suitable for the millimeter range. The new type of isolator employed is based on textured hexagonal ferrite materials, namely  $\text{BaNi}_2\text{Sc}_x\text{Fe}_{16-x}\text{O}_{27}$ . The net gain within the tuning band is 20-35 dB. The instantaneous bandwidth at a -3-dB level is 150-100 MHz, depending on the net gain. The noise temperature at the input does not exceed 25° K.

### I. INTRODUCTION

Making use of the results obtained earlier in the analyses of millimeter-band active crystals [1], the slow-wave structure [2], and ferrites [3], a traveling-wave maser (TWM) has been developed for the frequency range 40 to 46.5 GHz, which is char-

Manuscript received March 31, 1982; revised October 8, 1982. The authors are with the Institute of Radiophysics and Electronics, Academy of Sciences of the Ukrainian S.S.R., Kharkov, U.S.S.R.

acterized by a high value of the gain and a broad band of amplified frequencies. The preliminary results on this amplifier reported earlier in [4], [5] concerned mainly the higher frequency part of the above frequency range. The present paper contains new experimental results obtained in further investigations, particularly on measurements of the amplifier performance in the SWS passband.

The amplifier employs a number of novel elements, such as andalusite ( $\text{Al}_2\text{SiO}_5$ ) with  $\text{Fe}^{3+}$  ions as an active crystal, the  $\text{Ni}_2\text{W}$  hexaferrite for an isolator, and a comb-type slow-wave structure with smooth transitions to waveguides and other functional elements.

The general appearance of the maser is shown in Fig. 1.

### II. ACTIVE CRYSTAL, SLOW-WAVE STRUCTURE, AND ISOLATOR

The maser employs a natural  $\text{Fe}^{3+}$  containing crystal of andalusite operating in a magnetic field  $B_0$  oriented at 90° to the  $z$  axes of both magnetic complexes of the crystal. The axis  $z_1$  of one complex is along the SWS while  $z_2$  of the other is at 59° to  $z_2$ , both axes being perpendicular to  $B_0$ . The transition 1-2 is employed as a signal transition. One could pump the transitions 1-3 or 1-4 (see Fig. 2) which are but slightly different in frequency (1-2 GHz). The concentration of  $\text{Fe}^{3+}$  ions in the crystal is ~0.07 percent. The EPR bandwidth at the signal frequency is  $\Delta f_L = 150$  MHz, and at the pumping frequency

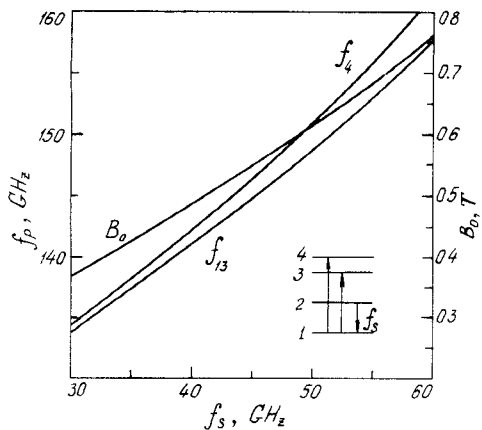
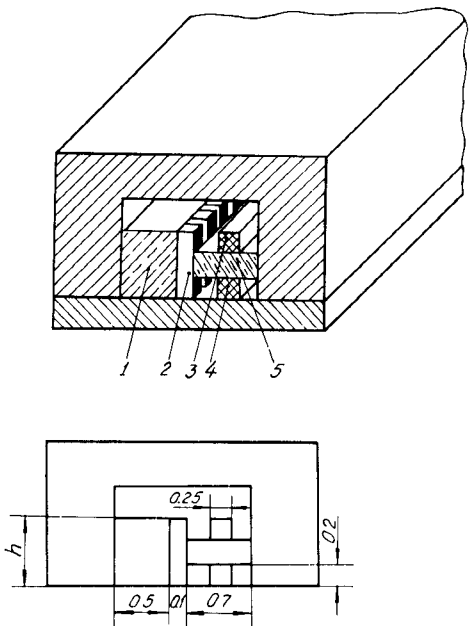
Fig. 2. Transition frequencies versus the applied magnetic field for  $\theta = 90^\circ$ .

Fig. 3. Cross section of the TWM slow-wave structure. 1-active crystal; 2-combs; 3-ferrite plate (isolator); 4-additional ferrite plate; 5-alumina plate.

$\Delta f_L^{(p)} \geq 500$  MHz. Data of the inversion coefficient  $I$  and the imaginary part of the inverted magnetic susceptibility  $|\chi''|$  are given in [1], [4]. Here we just note that these parameters of andalusite exceed such of ruby, rutile, or emerald as  $|\chi''| \geq 0.1$ , and the product  $m = |\chi''| \Delta f_L = 7-15$  MHz (at  $T = 1.7-2^\circ$  K).

The active crystal type usually dictates that of the SWS. In the present case, two factors dominated the choice, i.e., the relatively low value of the dielectric constant of andalusite ( $\epsilon = 8$ ) and the small amount of the material. Therefore, we have chosen a comb-type SWS. The main feature of the structure is the smooth transition to the waveguide [6], providing broad-band matching at both the signal and the pumping frequencies,  $f_s$  and  $f_p$ . Besides, "digits" of the structure have been shifted from the cavity center in order to improve performance of the isolator (Fig. 3). The digit height  $h$  is 0.8–0.9 mm, the structure period  $D$  is 0.3 mm, and the separation between the digits  $d$  is 0.15 mm. The group velocity slowing factor  $S$  equals  $\approx 20$ . A characteristic feature of the structure is the influence exerted by the magnetic field  $B_0$  on its dispersion at the propagation of a reflected wave through the SWS. This effect is caused by the influence of the ferrite magnetic properties on electrodynamic performance of the structure. How-

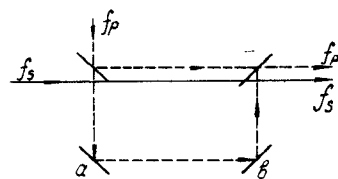


Fig. 4. The Zender-Mach interferometer setup.

ever, in the middle of the SWS passband, near the resonance magnetic field value, this gyrotropic perturbation is small. The effect will be considered in more detail (both theoretically and experimentally) in another paper.

The isolator of the TWM has been developed on the basis of textured hexagonal ferrite materials like  $\text{BaNi}_2\text{Sc}_x\text{Fe}_{16-x}O_{27}$  (often designated as  $\text{Ni}_2\text{W}$ ). Concentration and temperature dependences of the anisotropy fields,  $B_A$ , have been obtained for these ferrites, and the frequency-field dependences measured for ferrite plates of different cross-sectional geometries.

The broad FMR band of the ferrite (i.e., 2–3  $k0e$ ) results in a necessity of increasing the ferrite volume in the SWS which, in its turn, leads to an increased inhomogeneity of the dc magnetic field in the active material. In order to reduce the field nonuniformity and be able to control the magnetic field distribution, an additional ferrite plate was used (Fig. 3). The field nonuniformity in the SWS modified the basic relations for the electronic gain  $G_e$  (dB) and the instantaneous bandwidth at the  $-3$ -dB level,  $\Delta f_{1/2}$ . With an assumption that the EPR band remains Lorentzian, these take the form

$$G_e(\text{dB}) = 27.3S \frac{l}{\lambda} \frac{|\chi''|}{n} \eta \quad (1)$$

$$\Delta f_{1/2} = \Delta f_L \cdot n \sqrt{\frac{3}{G_e(\text{dB}) - 3}} \quad (2)$$

where  $n$  is the number characterizing the EPR line broadening,  $\eta$  is the crystal utilization factor, and  $l$  is the crystal length.

Equations (1) and (2) are approximate estimates, since the EPR line of an active crystal in a SWS does not just broaden but changes its form getting flatter near the top, which results in a flattened amplitude versus frequency curve of the amplifier.

Besides, the increased amount of the ferrite in the SWS brings about another important effect, i.e., a shift in the resonance field value of the forward wave against the FMR field of the reflected (backward) wave, which effect results in reduced total losses of the forward wave in the structure.

### III. PUMPING

The problem of guiding and injecting the pumpwave in the SWS with an active crystal arises in all quantum amplifiers. It becomes particularly complicated in the millimeter range where one faces the necessity of seeking other solutions than in the centimeter-wave masers.

We have suggested and implemented the following solution of the problem. The pumpwave is injected, through a Zender-Mach interferometer (ZMI) [7], into the signal channel, further guided in that channel to be introduced into the SWS.

The signal channel is a waveguide of a  $23 \times 10$ -mm $^2$  cross section. The ZMI also has been constructed in a guide of that cross section, hence the wave  $f_s$  passes the ZMI practically without interacting with it as an interferometer. The power at  $f_p$  can be directed to the signal waveguide if fed in an appropriate arm of the ZMI (Fig. 4). The losses at  $f_s$  change but weakly as the

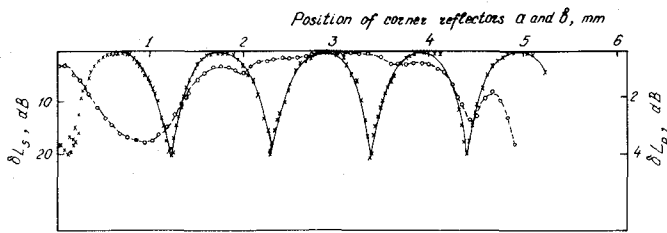


Fig. 5. Dependences of  $\delta P_s$  (°) and  $\delta P_p$  (x) on the position of the corner reflectors in ZMI.

frequency is changed over the entire tuning range, their magnitude remaining close to the minimum value (1 dB). The minimum losses in the ZMI at the pumping frequency are about 1.8–2 dB and seem to be reducible. Fig. 5 shows variations of both the signal and the pump wave ( $\delta P_s$  and  $\delta P_p$ , respectively) having passed the ZMI, depending on the position of the corner reflectors  $a$  and  $b$  (Fig. 4). The isolation of arms 3 and 1 is about 20 dB at  $f_p$ . This is of considerable importance, for the ZMI should be placed best at the maser output in order to decrease noise temperature (with that configuration adopted, the direction of the wave signal in Fig. 4 should be reversed). A wafer-type filter at the maser output, after the ZMI, provides for a better filtration of the pumping power. The source of pumping power is a diffraction radiation generator for 135–150 GHz yielding an output power about 1–2 W developed at the Institute of Radiophysics and Electronics, Academy of Sciences of the Ukrainian SSR [8].

#### IV. AMPLIFIER PERFORMANCE

By the time we had completed embodying our traveling wave maser with andalusite, authors in the field had published papers on similar devices employing ruby [9] and rutile [10] that operated in the same 8-mm range and were characterized by instantaneous bandwidths below  $\Delta f_{1/2} = 60$  MHz.

The andalusite-based TWM that has been developed operates in the range 40 to 46.5 GHz. The tuning band can be extended either towards lower frequencies or above 53–55 GHz. The range between 47 and 53 GHz is “forbidden” for operation with the chosen crystal orientation because of the harmonic cross relaxation [1]. To extend the amplification band in an operable maser, it is sufficient to either replace the ferrites or compose the isolator of ferrite plates of several marks. For adjusting the maser to frequencies above 53 GHz, it is necessary to reduce the height of SWS digits to  $h < 0.8$  mm and employ hexaferrites with higher values.

With the crystal length  $l = 20$  mm, the electron gain was  $G_e = 30$ –42 dB at  $T = 1.7$  K. The overall losses in the amplifier  $L_\Sigma$ , including such in the SWS, the waveguide with transitions and the ZMI do not exceed 10 dB at most frequencies of the passband, increasing only at the low frequency edge of the band (Fig. 6). Thus, the gain is  $G = 20$ –35 dB. The instantaneous band of the frequencies amplified varies between  $\Delta f_{1/2} = 150$  and 100 MHz, depending on the gain (Fig. 7). A property of the amplitude versus frequency curve is the flattened shape near the top, with the general broadening of the amplification band. This is in a good qualitative and quantitative agreement with the theoretical analysis of the maser performance, with an account of nonuniform dc and microwave fields in the active crystal volume. At some frequencies from  $\Delta f_{1/2}$ , the amplitude versus frequency curve shows a nonuniformity though remaining within  $\pm 3$  dB. It is due to features of the guiding channel and the interferometer, and peculiarities of the guide-SWS matching. The amount of nonuniformity increases at the low frequency edge of the band.

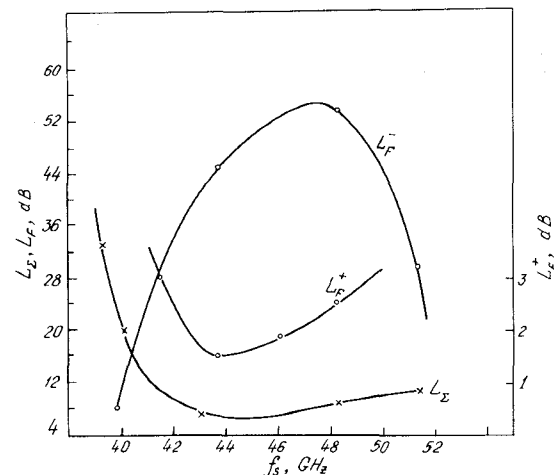


Fig. 6. Total losses ( $L_\Sigma$  dB) and the attenuation of the forward ( $L_F^+$  dB) and reflected ( $L_F^-$  dB) waves in the isolator versus the signal frequency  $f_s$ .

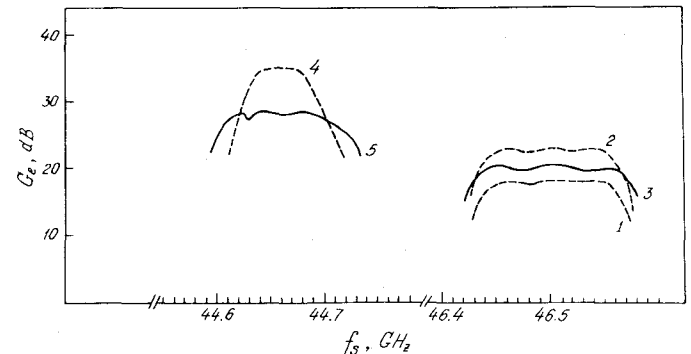


Fig. 7. Gain responses of the andalusite TWM in the tuning range. 1, 4, and 5-pump frequency  $f_p = f_{14}$ ; 2 and 3-pump frequency  $f_p = f_{13}$ .

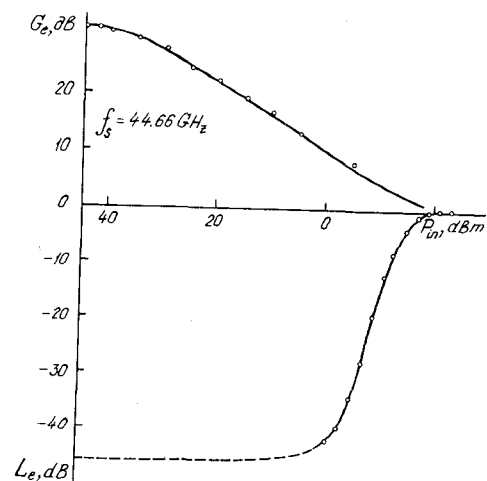


Fig. 8. Dependences of the electronic gain and absorption on the input signal amplitude.

The instantaneous bandwidth of the amplifier can be rather simply controlled by slightly changing the orientation of the magnetic field  $B_0$  with respect to the crystal (see Fig. 7).

We have also measured the dependences of  $G_e$  and  $L_e$ , the paramagnetic absorption, on the input amplitude (Fig. 8) and found a difference in their saturation curves. The effect was earlier investigated theoretically [11].

The nominal noise temperature brought to the maser input does not exceed 25° K.

## V. CONCLUSION

Thus, our efforts have resulted in the implementation of a millimeter-range traveling-wave maser using andalusite which at the moment of work completion was the shortest-wavelength maser of its type.

Recently, we have become aware of a rutile maser operating at even shorter wavelengths [12].

Currently, our maser is the most wide-band TWM of the millimeter range supposedly to become useful for spectral and radiometric applications.

The physical results obtained suggest the possibility of a further extension of the amplification band, to several hundred megahertz, and shortening of the operation wavelength to  $\lambda < 3$  mm.

Since the end of 1981, the maser has been employed as an amplifier in the radio telescope RT-25×2 (Institute for Applied Physics, Academy of Sciences of the U.S.S.R., Gorky).

## ACKNOWLEDGMENT

The authors wish to express their gratitude to L. I. Fedoseev (Institute for Applied Physics, Academy of Sciences of the U.S.S.R.) who has developed the Zender-Mach interferometer placed at our disposal by courtesy of Dr. A. G. Kislyakov.

It is a pleasure to thank Dr. E. L. Kollberg of the Chalmers University of Technology in Göteborg, Sweden for having sent us a technical report on the rutile traveling-wave maser.

## REFERENCES

- [1] N. T. Cherpak, "Cross relaxation in inverted spin system of three-valence iron ions in andalusite," *Solid State Phys. (Fizika Tverdogo Tela, USSR)*, vol. 22, pp. 3539-3543, Dec. 1980 (in Russian).
- [2] N. T. Cherpak, A. A. Lavrinovich, V. V. Mishchenko, and T. A. Smirnova, "Investigation of comb-type retarding structure for millimeter-band maser," *Radioelectron. and Communicat. Syst. (Izv. VUZ Radioelectron., USSR)*, vol. 24, pp. 9-14, December, 1981 (in Russian).
- [3] V. I. Ivanova, L. N. Kolpakova, I. I. Petrova, T. A. Smirnova, and N. T. Cherpak, "Investigation of hexagonal ferrites  $Ni_2Sc_xW$  by FMR method throughout the temperature range 300-4.2° K," *Magnetic Resonance and Related Phenomena* (Proc. XXth Congr. Ampere, Tallinn, USSR, Aug. 21-26, 1978). Berlin, Heidelberg, New York: Springer, 1979, p. 371.
- [4] N. T. Cherpak, V. V. Mishchenko, S. A. Peskovskii, and T. A. Smirnova, "Andalusite traveling-wave maser in the millimeter wavelength range," *Dokl. Akad. Nauk Ukr. SSR* (in Russian), ser. A, pp. 69-71, Feb. 1980.
- [5] N. T. Cherpak, T. A. Smirnova, V. V. Mishchenko, S. A. Peskovskii, and A. A. Lavrinovich, "Traveling wave maser in 6-mm wave band with instantaneous bandwidth exceeding 100 MGz," in *III All-Union Sym. Millimeter and Submillimeter Waves*, September, 22-24, 1980, Gorky, Inst. Applied Phys., Acad. Sciences of the USSR, 1980, pp. 23-24.
- [6] L. I. Marchenko, V. V. Mishchenko and N. T. Cherpak, "Broad-band matching in the traveling-wave paramagnetic amplifier," *Radioelectron. and Communicat. Syst. (Izv. VUZ Radioelectron., USSR)*, vol. 22, pp. 75-76, Sept. 1979 (in Russian).
- [7] L. I. Fedoseev and Yu. Yu. Kukhov, "Superheterodyne radiometers of millimeter and submillimeter wavebands," *Radio Eng. El. Phys. (Radio-tehnika i elektron., USSR)*, vol. 16, pp. 554-560, Apr. 1971, (in Russian).
- [8] V. P. Shestopalov, *Difraktsionnaja Elektronika*. Kharkov: State University, 1976 (in Russian).
- [9] V. I. Zagatin, G. A. Misezhnikov, and V. B. Shteinglyer, "Ruby maser operating in the 8-mm range," *Radio Eng. El. Phys.*, vol. 12, pp. 501-502, Mar. 1967.
- [10] E. L. Kollberg and P. Th. Lewin, "Traveling wave masers for radio astronomy in the frequency range 20-40 GHz," *IEEE Trans. Microwave Theory Tech.*, vol. MTT-22, pp. 718-725, Nov. 1976.
- [11] N. T. Cherpak, "Amplification and absorption of an electromagnetic wave in slowing structure with a paramagnetic crystal," *Izv. VUZ Radiofizika (USSR)*, vol. 22, pp. 819-825, July 1979 (in Russian).
- [12] T. C. L. G. Sollner, D. P. Clemens, T. L. Korzeniowski, G. C. McIntosh, E. L. Moor, and K. S. Yngvesson, "Low-noise 86-88 GHz traveling wave maser," *Appl. Phys. Lett.*, vol. 35, pp. 833-835, Nov. 1979.

## A Note Concerning Modes in Dielectric Waveguide Gratings for Filter Applications

GEORGE L. MATTHAEI, FELLOW, IEEE

**Abstract**—Peng and Oliner, and others have shown that TM-to-TE or TE-to-TM mode conversions occur when a single, lowest order surface wave is incident obliquely onto a wide dielectric grating and that the lowest order converted modes of this sort can cause spurious stopbands which are especially troublesome because they are so close to the desired stopband. In this note it is observed that the spurious response situation is not as bad in the case of a grating cut into a dielectric waveguide (which can be thought of as having two, obliquely incident waves present). In this latter case, the fields have even or odd symmetry which eliminates part of the mode couplings including the lowest order TM-to-TE or TE-to-TM couplings. Experimental and theoretical results indicate that gratings can be made to be free from spurious responses or appreciable radiation over sizeable bands so that they can be useful in at least some kinds of dielectric waveguide filter structures.

## I. BACKGROUND

Peng, Oliner, and their coauthors have made extensive studies of propagation effects in dielectric waveguides [1], [2]. In particular, they show that TE-to-TM (or TM-to-TE) mode conversion at the side walls of a uniform guide can result in leakage and other effects not apparent from the often used approximate theories. In this context it should be noted that by a "TE" mode they mean that the waveguide mode can be thought of as being predominantly composed of two obliquely traveling TE surface waves as suggested on the left in Fig. 1(a), and analogously for "TM" modes. Their analysis shows that when a surface wave strikes a vertical edge at an oblique angle, the boundary conditions result in some conversion of the incident surface wave from its original wave type to the opposite wave type. As a result, the waves cannot be purely TE or purely TM in character, and in certain types of uniform dielectric waveguide structures leakage may exist which might not be expected from conventional points of view [2].

In [3], the analysis described above is extended to the case of dielectric waveguides with arrays of grooves added as suggested to the right in Fig. 1(a), and also wide gratings as in Fig. 1(b). (Gratings as in Fig. 1(a) are of potential interest for use in filters among other applications.) Let us for the moment consider the case of a wide grating with a single-wave incident as suggested in Fig. 1(b). If a lowest order TM mode is incident, the TM-to-TE conversion in the grating may result in the generation of an independent, lowest order TE bound mode in addition to the initial TM mode. Such a bound TE mode could be quite troublesome as it could have a phase velocity only slightly different from that of the incident TM wave, and it could create an unwanted, spurious, grating stopband quite close in frequency to the desired grating stopband.

In [4], an effect such as that described above is demonstrated experimentally for the case of a laser beam incident at an oblique angle onto a grating much wider than the incident beam as in Fig. 1(b). With a TE surface-wave beam incident, a stopband was observed due to the TE wave along with an overlapping, strong stopband due to the TM wave generated in the grating by

Manuscript received June 3, 1982; revised September 9, 1982. This research was supported by the National Science Foundation under Grant ECS-8016720. The author is with the Department of Electrical and Computer Engineering, University of California, Santa Barbara, CA 93106.